

Noninvasive fMRI Investigation of Interaural Level Difference Processing in the Rat Subcortex

Condon Lau^{1,2}, Jevin W. Zhang^{1,2}, Joe S. Cheng^{1,2}, Kyle K. Xing^{1,2}, Iris Y. Zhou^{1,2}, Matthew M. Cheung^{1,2}, and Ed X. Wu^{1,2}

¹Laboratory of Biomedical Imaging and Signal Processing, The University of Hong Kong, Hong Kong, Hong Kong SAR, China, People's Republic of, ²Department of Electrical and Electronic Engineering, The University of Hong Kong, Hong Kong, Hong Kong SAR, China, People's Republic of

Introduction: Mammals can determine the angular position of an object by its sounds. This ability is known as sound localization [1]. Acoustic pressure waves arriving from different directions are altered by the head and pinnae before entering the ear canals. Sounds from different azimuths (angle along the horizontal plane) arrive at the ears with different sound pressure levels (SPL). This is known as interaural level difference (ILD) and is an important feature for sound localization. ILD processing has been extensively studied with invasive techniques, which show subcortical structures play a significant role. Noninvasive BOLD fMRI can examine the entire brain simultaneously and thus, significantly improves comparisons between structures and brain hemispheres. In this study, we examine a rat ILD model using fMRI. Human studies have examined ILD processing in the cortex [2], but human subcortical structures are small and thus, more difficult to image. The rat subcortex occupies a significantly larger portion of the brain and is suited to fMRI studies.

Materials and Methods: Experimental methods were detailed in our previous publications [3] and this section will focus on new methods. **Animal preparation** Normal male SD rats (n=6) were anesthetized and key vital signs were monitored. **Auditory stimulation** The block-design stimulation paradigm consisted of four blocks of 20s acoustic noise stimulation (amplitude modulated at 8Hz and 92% duty cycle) and 40s silence. The stimuli were produced using ultrasonic loudspeakers (Kemo Electronic L010) driven by waveform generators (HP 33120A). Sound was transmitted via delivery tubes which entered the ear canals. Seven ILD settings from -18 (right ear SPL higher than left ear SPL) to +18dB in 6dB increments were used. The SPL at ILD = 0dB was 86dB in each ear. ILD was changed by changing the left and right ear SPLs by equal and opposite amounts. **fMRI protocol** Experiments were performed using a 7T scanner (Bruker PharmScan). Single-shot SE-EPI images (TR/TA/TE = 2000/1000/43ms, FOV = 32x32mm², matrix = 64x64, four 1mm thick slices with 0.2mm gaps) were acquired throughout the experiment. **Data analysis** The fMRI images were realigned and smoothed (Wellcome Centre SPM8). Time series were analyzed using period cross-correlation (CMRR Stimulate6). Functionally defined ROIs were drawn in each hemisphere around structures along the auditory pathway by computing the r map after averaging all seven ILD settings. BOLD changes were computed from the average time series within each ROI by dividing the average signal during stimulation by the average signal from 5s before to onset of stimulation (baseline) and expressing the quotient as a percentage of baseline. BOLD change ratios were computed by dividing the left hemisphere change by the right hemisphere change. We represent the fMRI response amplitude in units of BOLD change, which equal 100% + conventional % change units, because the BOLD change ratios remain positive even if the BOLD change in one hemisphere is small.

Results and Discussion: Activated structures in Fig. 1 include the cochlear nerve (CoN), cochlear nucleus (CN), superior olivary complex (SOC), ventral and dorsal lateral lemnisci (VLL and DLL), inferior colliculus (IC), and crus 1 of the ansiform lobule (Crus1). ROIs were drawn around voxels with $r > 0.22$ in each structure except for the CoN and Crus1. The CoN is in an area of high susceptibility gradients and the Crus1 BOLD response is not consistent across animals. The activated structures are all known components of the rat auditory pathway [3,4,5]. In Fig. 2, the DLL and IC responses shift contralateral to the higher SPL ear at non-zero ILD settings while the CN, SOC, and VLL responses do not shift noticeably from symmetry. The BOLD changes (averaged across hemispheres) at ILD = 0dB are 100.90% (CN), 101.26% (SOC), 101.14% (VLL), 100.61% (DLL), and 101.10% (IC) of baseline. When the BOLD change ratios in Fig. 3 are fitted to lines, the slopes are (units dB⁻¹) 1.2×10^{-4} (CN), -1.8×10^{-4} (SOC), -1.8×10^{-4} (VLL), -3.4×10^{-4} (DLL), and -7.0×10^{-4} (IC). Tables 1 and 2 show the statistical significance of change ratio comparisons in the IC and DLL. The SOC ratios at -12dB and +12dB are also significantly different ($p < 0.05$). All other comparisons did not yield significant differences. These trends agree with invasive findings. The SOC receives inhibitory and excitatory inputs from the contralateral and ipsilateral CNs, respectively, and performs "subtraction" to process ILDs [1]. The CN is upstream of the SOC and therefore, its change ratio does not vary directly with ILD. The SOC ratio's ILD dependence is reduced by the competing inhibitory and excitatory inputs. The VLL, DLL, and IC are downstream of the SOC and thus, their ratios are inversely related with ILD (note this study does not observe a significant trend in the VLL), in accordance with invasive findings [6,7].

Conclusions: The IC and DLL contralateral to the higher SPL ear respond with larger BOLD change. This asymmetry is not apparent in the CN and SOC. Future studies can examine different sound conditions, animal injury/plasticity models, and other mechanisms of sound localization such as subcortical processing of spectral distortions and arrival time differences at the two ears.

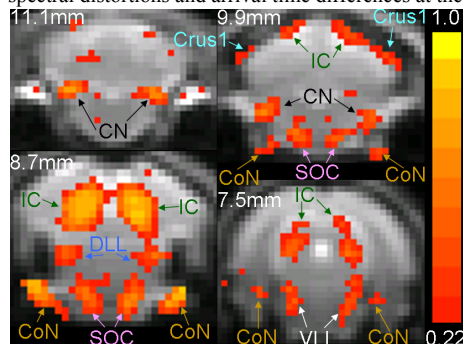


Figure 1: r map computed from a representative animal after averaging all seven ILD settings. Each coronal slice's distance from Bregma is shown (larger numbers more posterior).

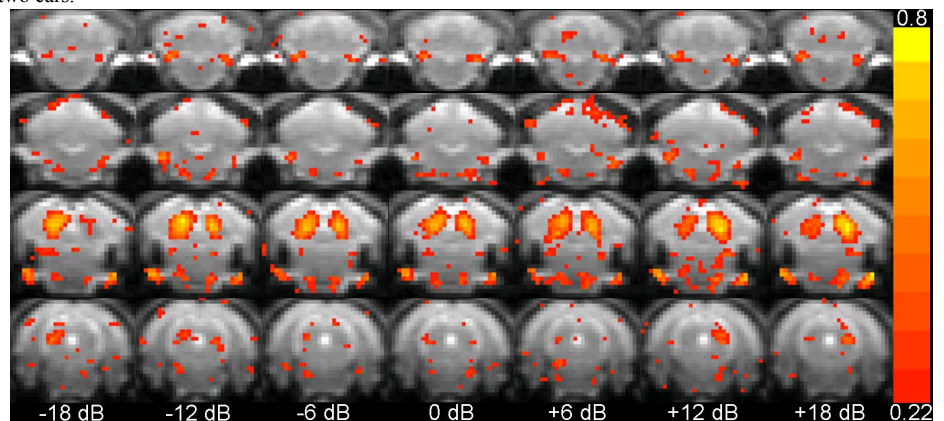


Figure 2: r maps at seven ILD settings (columns) computed from the representative animal in Fig. 1.

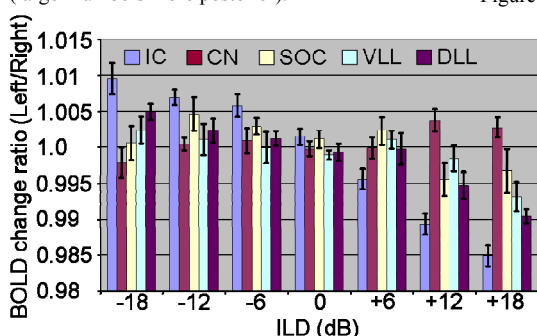


Figure 3: Mean and standard error of BOLD change ratios acquired from structures along the auditory pathway.

References: [1] Grothe B *et al.*, *Physiol Rev*, 2010. [2] Smith KR *et al.*, *Neuroreport*, 2004. [3] Cheung MM *et al.*, *ISMRM*, 2011. [4] Woody CD *et al.*, *Neuroscience*, 1999. [5] Yu X *et al.*, *ISMRM*, 2009. [6] Irvine DR *et al.*, *Hear Res*, 1995. [7] Kelly JB *et al.*, *Hear Res*, 1998.

		ILD (dB)						
ILD (dB)	IC	-18	-12	-6	0	+6	+12	+18
	-18	-	NS	NS	**	***	***	***
	-12	NS	-	NS	NS	***	***	***
	-6	NS	NS	-	NS	***	***	***
	0	**	NS	NS	-	*	***	***
	+6	***	***	***	*	-	NS	**
	+12	***	***	***	***	NS	-	NS
	+18	***	***	***	***	**	NS	-

		ILD (dB)						
ILD (dB)	DLL	-18	-12	-6	0	+6	+12	+18
	-18	-	NS	NS	NS	NS	**	***
	-12	NS	-	NS	NS	NS	*	**
	-6	NS	NS	-	NS	NS	*	**
	0	NS	NS	NS	-	NS	NS	**
	+6	NS	NS	NS	NS	-	NS	NS
	+12	**	*	*	NS	NS	-	NS
	+18	***	**	**	**	NS	NS	-

Tables 1 and 2: P-value tables computed from the IC (1) and DLL (2) BOLD change ratios in Fig. 3. NS, *, **, and *** indicate $p > 0.05$, $p < 0.05$, $p < 0.01$, and $p < 0.001$, respectively. All calculations were performed with one-way, repeated measures ANOVA and Tukey's test.